biotin-streptavidin linkages. Because the linkage length is <1% that of the microtubule, the observed pivoting must occur around an axis inclined no more than ~2° from the surface normal. Because individual linkages presumably project from the surface over a broader range of inclination angles, the observation that all microtubules pivot around the surface normal through similar angular ranges suggests that the linkage has a significant bending compliance.
28. Measurement of K from thermal fluctuations requires that the orientational correlation time be much longer than the single-frame acquisition time. We verified that this requirement was fulfilled by confirming that the variance of randomly selected data records was reduced by <10% when angle records sampled at 30 Hz were filtered with a four-point mean filter. For some microtubules, small (~11° to 22°) stochastic shifts in the equilibrium position occurred at ~50-s intervals, increasing the measured variance. Thus, the calculated value of K somewhat underestimates the true stiffness of the microtubule-kinesin–cover slip linkage.
29. Torsional stiffness of similar magnitude was previously observed in single-molecule measurements of the orientation of F-actin attached to the F_1-ATPase (*35*). As in our experiments, the filament-surface linkage in that study includes a coiled coil (the γ subunit) and a biotin-streptavidin linkage.
30. The relaxation time is calculated as $\tau = (1/3)c_\perp(L_1^3 + L_2^3)/K$, where $c_\perp = 9.4 \times 10^{-3}$ N s m^{-2} is the drag coefficient per unit length for translation perpendicular to the microtubule axis and L_1 and L_2 are the lengths of the two ends of the microtubule (*26*). The median τ values for microtubules in the 1 mM AMP-PNP, 400 nM ATP, and 5 nM ATP experiments reported here are 1.0 ± 1.4, 0.8 ± 1.3, and 0.2 ± 0.6 (± SD) s. These values are consistent with independent estimates of the relaxation times derived from autocorrelation analysis of the microtubule orientation records.
31. W. Hua, J. Chung, J. Gelles, manuscript in preparation.
32. J. Chung, W. Hua, J. Gelles, manuscript in preparation.
33. A. Hoenger *et al.*, *J. Mol. Biol.* **297**, 1087 (2000).
34. K. Svoboda, C. F. Schmidt, B. J. Schnapp, S. M. Block, *Nature* **365**, 721 (1993).
35. H. Noji, R. Yasuda, M. Yoshida, K. Kinosita Jr., *Nature* **386**, 299 (1997).
36. Unlabeled microtubules were visualized by differential interference contrast microscopy, movements were recorded on videotape (30 frames s^{-1}), and the positions of both microtubule ends were measured in single frames, as described (*7*). The measured end positions were then used to compute the orientation of the microtubule relative to an arbitrary reference orientation. Microtubules were chosen for analysis only if the pivot point remained sufficiently far from the center or the torsional relaxation time was sufficiently long that the two ends could be unambiguously distinguished. Orientations were typically measured at ~1-s intervals, but the sampling interval was occasionally reduced to 33.3 ms to verify reliable end tracking.
37. A movie showing microtubule movement under this condition is available as supplementary material on *Science* Online at www.sciencemag.org/cgi/content/full/295/5556/844/DC1.
38. The position of the microtubule pivoting point at time $t(i)$ was measured from the intersection of microtubule traces (reconstructed from the end positions) from two neighboring frames. If the microtubules in the neighboring frames were parallel, the first frame was excluded from further analysis. The length of each end of the microtubule at time $t(i)$ was then calculated as the microtubule end-to-pivot-point lengths $L_1(i)$ and $L_2(i)$. Time courses of L_1 and L_2 were used to calculate microtubule end velocities v_1 and v_2 by linear regression. Translation velocity was taken to be $|(v_1 - v_2)/2|$; the absolute value was computed because the polarity of the microtubules was not independently determined in these experiments. The use of the absolute value in this calculation results in a small positive bias in velocity measurements on nonmoving microtubules (e.g., those in AMP-PNP).
39. We thank E. Young and C. Ding for the initial assay development, A. Hiller for painstaking analysis of microtubule orientation data, and E. Young, L. Hedstrom, C. Miller, M. Welte, and K. Kinosita Jr. for comments on the manuscript. Supported by the National Institute of General Medical Sciences.

4 June 2001; accepted 19 December 2001

Partitioning of the Matrix Fraction of the Golgi Apparatus During Mitosis in Animal Cells

Joachim Seemann, Marc Pypaert, Tomohiko Taguchi, Jörg Malsam, Graham Warren*

The Golgi apparatus is partitioned during mitosis in animal cells by a process of fragmentation, dispersal, and reassembly in each daughter cell. We fractionated the Golgi apparatus in vivo using the drug brefeldin A or a dominant-negative mutant of the Sar1p protein. After these treatments, Golgi enzymes moved back to the endoplasmic reticulum, leaving behind a matrix of Golgi structural proteins. Under these conditions, cells still entered and exited mitosis normally, and their Golgi matrix partitioned in a manner very similar to that of the complete organelle. Thus, the matrix may be the partitioning unit of the Golgi apparatus and may carry the Golgi enzyme–containing membranes into the daughter cells.

There are two popular models of the partitioning of the Golgi apparatus during mitosis in animal cells, which differ as to the nature of the partitioning units. The first model argues that the units are the Golgi membranes themselves, which break down at the onset of mitosis, yielding vesicle clusters and shed vesicles, either or both of which have been suggested as the means of inheriting the Golgi (*1–4*). The second model argues that the partitioning units are endoplasmic reticulum (ER) membranes, with the Golgi merging with the ER during prometaphase and emerging from it during telophase (*5*).

Attempts to distinguish between these two models have yielded contradictory results, particularly when Golgi enzymes have been used to trace the partitioning process (*1–3*, *5–7*). We therefore decided to focus on another class of markers, the Golgi matrix proteins, which include the golgin and GRASP families of vesicle tethering and cisternal stacking proteins (*8*). In the presence of brefeldin A (BFA), these matrix proteins can be separated from Golgi enzymes (*9*). The enzymes move to the ER, whereas matrix proteins appear in dispersed punctate structures that may become associated with ER export sites (*10*). Separation also occurs in the presence of a dominant-negative Sar1p protein, which traps the Golgi enzymes as they cycle through the ER (*1*, *5*, *11*, *12*). The matrix proteins slowly disperse throughout the cytoplasm, although there is evidence that some become associated with the ER (*13*), especially when a guanosine diphosphate–restricted form of a dominant-negative Sar1p is used (*10*).

When BFA-treated cells are injected with Sar1dn (a guanosine triphosphate–restricted form) and the BFA is washed out, the matrix proteins re-form a ribbon-like structure near the nucleus that resembles the Golgi apparatus even though Golgi enzymes are trapped in the ER (*9*). This suggests that the matrix may provide a scaffold for the Golgi enzyme–containing membranes (*9*). The matrix might also provide the means of partitioning the Golgi during mitosis, so we asked whether it would partition between daughter cells in the absence of the enzyme-containing membranes that normally populate it. We first tested the effect of BFA on progression through mitosis, using time-lapse microscopy of synchronized normal rat kidney (NRK) cells. BFA had no effect on the time elapsed from prometaphase to telophase/G_1 [control cells, 32 ± 2 (SD) min; BFA-treated cells, 33 ± 2 (SD) min] when added about 90 min before the mitotic peak, which is sufficient time to separate enzyme and matrix proteins before entry into mitosis (*14*).

Unsynchronized cells were then treated with BFA for 90 min, fixed, and labeled for the Golgi matrix marker GM130, microtubules, and DNA, to determine the mitotic phase (*15*). After treatment with BFA, the matrix fraction of the interphase Golgi was a little more fragmented, but

Table 1. Distribution of GM130 in mitotic NRK cells. BFA was added, 90 min before fixation, to exponentially growing NRK cells, which were then labeled with polyclonal antibodies to GM130 and secondary antibodies coupled to Alexa Fluor 488. Total fluorescence on each side of the equatorial plate in metaphase cells and in each daughter cell pair in telophase was quantified, and background fluorescence was subtracted. For each pair of values, the percentage deviation from 50% was calculated, and the median deviation was determined from the number (n) of pairs evaluated.

	Median deviation from equality	
	+BFA	Control
Metaphase	2.8% (n = 87)	3.2% (n = 79)
Telophase/G_1	3.8% (n = 56)	3.7% (n = 57)

Department of Cell Biology, Ludwig Institute for Cancer Research, Yale University School of Medicine, 333 Cedar Street, Post Office Box 208002, New Haven, CT 06520–8002, USA.

*To whom correspondence should be addressed. E-mail: graham.warren@yale.edu

once the cells had entered mitosis, the behavior was very similar to that of untreated cells (Fig. 1) (*16*). From prophase to metaphase, the matrix fragments became increasingly associated with the two forming spindle poles. During anaphase, the fragments moved as a cohort with each of the separating sets of sister chromatids. During telophase, congregated fragments were present on both sides of each re-forming nucleus, the major pool being associated with the centrosomes and the minor pool being near to the mid-body. Similar results were obtained for other Golgi matrix markers, including the GRASPs (*17*).

The accuracy of partitioning was assessed

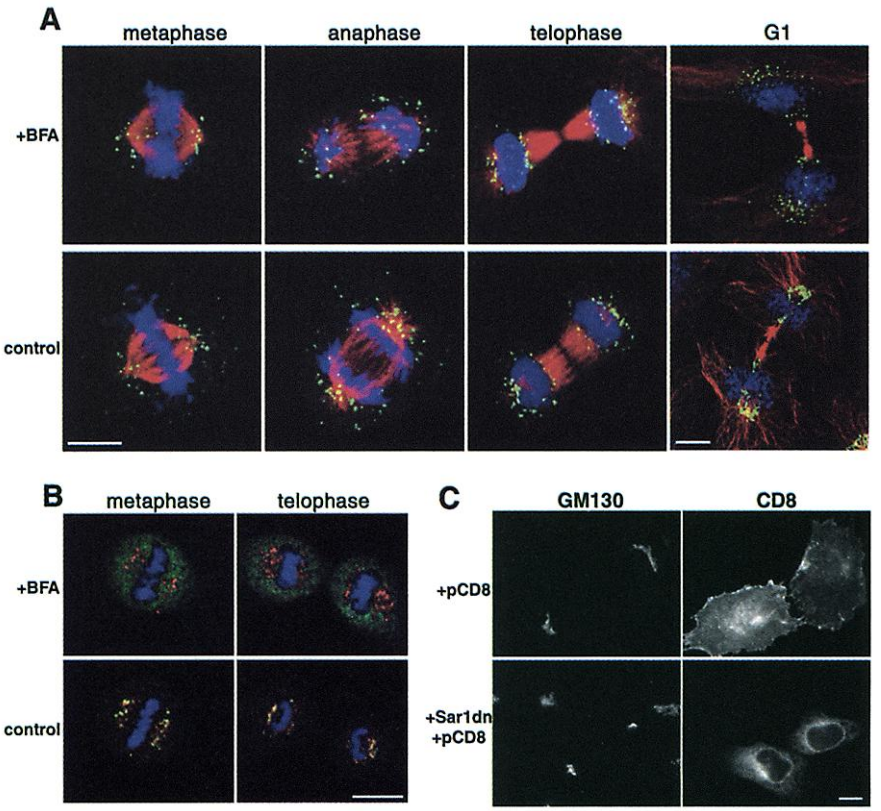

Fig. 1. Partitioning of matrix proteins in the presence and absence of BFA. (**A**) Exponentially growing NRK cells were treated with BFA 90 min before fixation (top panels) or left untreated (bottom panels), then triple-labeled for the matrix marker GM130 (green), α-tubulin (red), and DNA (TO-PRO3 iodine, blue). The cells shown are representative confocal fluorescence sections of cells at the indicated mitotic stages. Scale bar, 10 μm. (**B**) Cells are as in (A), but triple-labeled for GM130 (red), ManII (green), and DNA (blue). Scale bar, 15 μm. (**C**) BFA-treated NRK cells in metaphase were microinjected with a plasmid encoding the cDNA for CD8 alone (+pCD8) or together with Sar1dn protein (+Sar1dn +pCD8). BFA was washed out at the end of mitosis to allow reformation of the Golgi apparatus, and the cells were incubated for 2 hours and chased with cycloheximide before fixation and double-labeling with antibodies to GM130 and CD8. Scale bar, 15 μm.

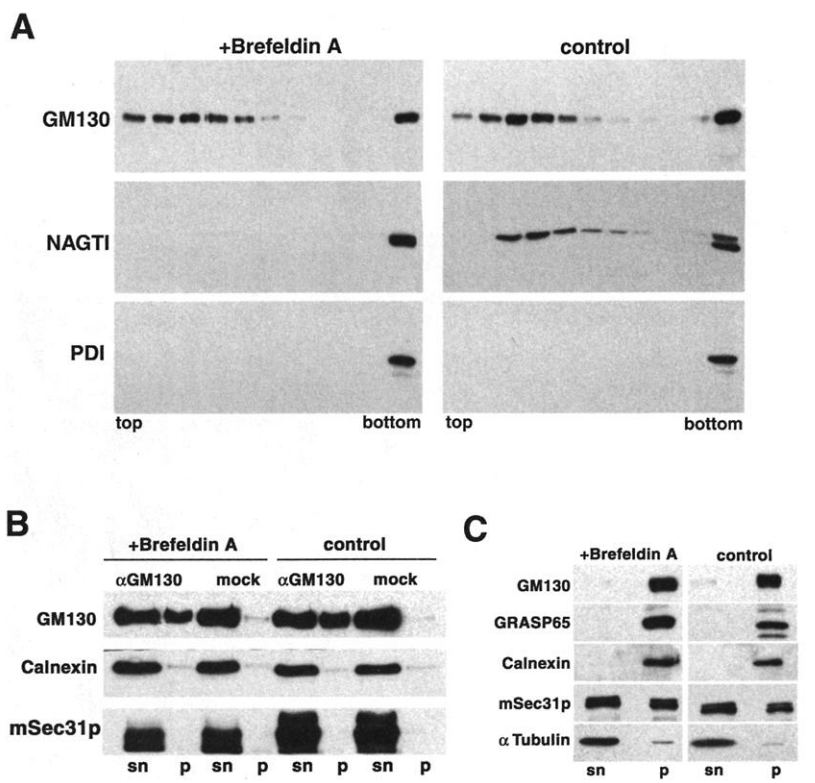

Fig. 2. Biochemical separation of Golgi enzyme and matrix components in mitotic cells treated with BFA. (**A**) Postchromosomal supernatants of mitotic HeLa cells (±BFA treatment) were fractionated on a velocity gradient, and fractions were analyzed by immunoblotting with antibodies against the matrix protein GM130, the Golgi enzyme NAGTI-myc, and the ER protein PDI. (**B**) Mitotic membranes containing GM130 were immunoisolated from a PCS of mitotic NRK cells (±BFA treatment) by means of magnetic beads coated (or not) with a monoclonal antibody against GM130. Equal fractions of the supernatant (sn) and washed pellet (p) were processed by Western blotting using the indicated antibodies. (**C**) Membranes were separated from cytoplasmic proteins by centrifugation of a PCS from mitotic HeLa cells (±BFA treatment). Equal fractions of the supernatant and pellet were analyzed by Western blotting using the indicated antibodies.

by measuring the amount of the matrix marker GM130 on each side of the equatorial plate in metaphase cells and in each daughter cell pair in telophase (*14*). The median deviation from equality was 2.8 to 3.8% for both control and BFA-treated cells (Table 1), further supporting the idea that matrix proteins alone can mediate accurate partitioning of the Golgi.

Cells were also double-labeled for GM130 and the Golgi enzyme mannosidase II (ManII) to show that BFA had relocalized Golgi enzymes to the ER before cells entered mitosis. Both markers mostly colocalized in untreated mitotic cells, but prior treatment with BFA selectively changed the pattern of ManII staining to that of the ER (*1*, *2*) (Fig. 1B).

This separation of enzymes from matrix proteins was corroborated by means of biochemical techniques. HeLa and NRK cells were prepared by shake-off (*18*), giving essentially the same results. A postchromosomal supernatant (PCS) was applied to a glycerol velocity gradient (*3*, *6*), and fractions were probed for ER and Golgi markers (*19*). ER membranes [marked by protein disulphide isomerase (PDI)] sedimented rapidly onto the sucrose cushion, whereas most of the Golgi enzyme [*N*-acetylglucosaminyltransferase I (NAGTI)] and matrix (GM130) markers sedimented more slowly (Fig. 2A). However, in the presence of BFA, the Golgi markers separated, with the enzyme NAGTI moving from the Golgi to the ER fraction. The sedimentation of the matrix marker GM130 was essentially unchanged.

A fraction of the Golgi always sedimented onto the sucrose cushion even in the absence of BFA (Fig. 2A). Linstedt and colleagues (*3*, *6*) have characterized this fraction, showing that the Golgi and ER membranes within it are distinct. We have also carried out cryo–electron microscopy (cryo-EM) studies showing that ~90% of the Golgi matrix marker GRASP65 did not colocalize with ER membranes, with or without BFA treatment. But to ensure that Golgi matrix and ER membranes were distinct in mitotic cells, we adopted an immunoaffinity approach using magnetic beads coated with antibodies to GM130 (*19*). These beads retrieved 30 to 40% of the GM130-containing membranes before or after treatment with BFA, whereas mock beads retrieved essentially none (Fig. 2B). In marked contrast, there was little if any retrieval of the ER membrane marker calnexin under either condition, showing that GM130 does not move to the ER in the presence of BFA. It was important to show that immunoisolated GM130 was membrane-bound and not free in the cytoplasm. This concern was raised by recent evidence suggesting that there is a sizable cytoplasmic pool of GRASP65 (*10*), the tightly bound partner of GM130 (*20*). However, in agreement with other results (*20*–*23*), we could find no evidence for such a pool because >98% of both GM130 and GRASP65 in mitotic cell extracts (±BFA) could be sedimented, as could the ER membrane marker calnexin (Fig. 2C). Tubulin provided the control cytoplasmic marker and did not sediment (*19*). Similar results were obtained for interphase cell extracts (*17*).

It has also been suggested that matrix proteins become part of ER export sites in interphase cells treated with BFA (*10*). The COPII coat protein mSec31p is often used as a marker for these sites (*24*), and about half of the mSec31p in mitotic cell extracts was bound to membranes, in agreement with quantitative EM analysis (*25*). This percentage was unchanged by treatment with BFA (Fig. 2C). Anti-GM130 beads did not retrieve any mSec31p under either condition (Fig. 2B), which strongly argues against the matrix proteins being part of modified ER export sites, at least in mitotic cells, and so being partitioned as part of the ER.

EM techniques were next used to study the partitioning matrix (*26*). In BFA-treated mitotic cells, the matrix contained embedded vesicles and tubules (Fig. 3A) similar to those seen in BFA-treated interphase cells (*9*). Morphologically similar structures could be labeled in cryosections with antibodies to GM130 (Fig. 3B). Smaller structures, including individual vesicles, were often labeled (Fig. 3B), which is consistent with some dispersal of the GM130 signal seen by fluorescence microscopy (Fig. 1) (*3*, *6*, *27*). Labeling for GM130 was not observed over ER membranes, which were often enlarged after

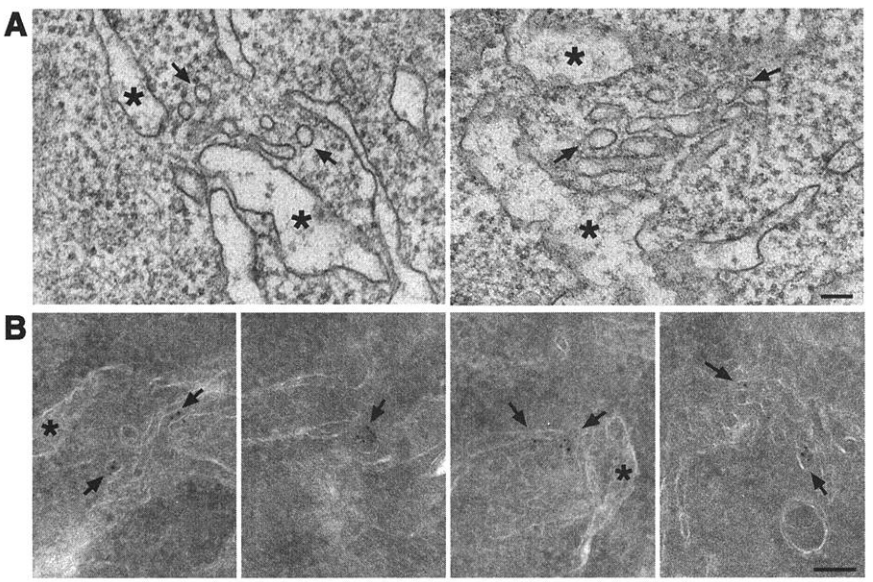

Fig. 3. Effect of BFA on the ultrastructure of mitotic Golgi membranes in NRK cells. Synchronized NRK cells were treated with BFA 90 min before fixation and preparation of Epon (**A**) or cryo-sections (**B**). The matrix fraction with embedded vesicles and tubules [(A), arrows] could be labeled with antibodies to GM130 (B) as could individual vesicles [second panel of (B)]. Note the swollen ER in the presence of BFA (asterisks). Scale bar, 100 nm.

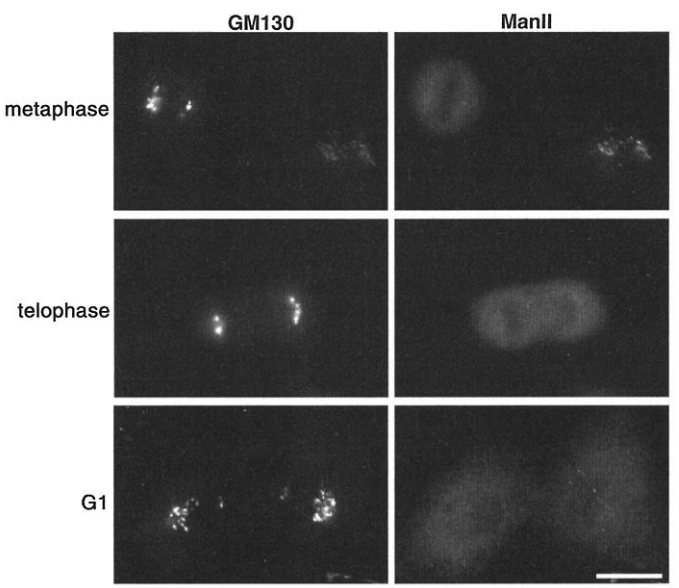

Fig. 4. Partitioning of matrix proteins in NRK cells injected with Sar1dn. Synchronized NRK cells were microinjected with Sar1dn 5 to 6 hours before entering mitosis, together with sheep IgG as a marker to identify injected cells. Cells were fixed at different time points and triple-labeled for GM130 (left panels), ManII (right panels), and sheep IgG (not shown). Scale bar, 15 μm.

BFA treatment, making them even easier to identify (Fig. 3, asterisks).

The partitioned matrix components were next tested for functionality. NRK cells that had entered metaphase in the presence of BFA were microinjected with a plasmid encoding the plasma membrane marker CD8 (*28*). After mitosis, BFA was washed out to permit repopulation of the Golgi matrix with enzyme-containing membranes. Two hours later, analysis showed that the re-formed Golgi mediated the transport of CD8 to the cell surface (Fig. 1C). As a control, co-injection of Sar1dn (*29*) prevented exit from the ER, even though the matrix components re-formed a ribbon-like structure.

As an alternative to BFA, we used Sar1dn to fractionate the Golgi apparatus. Synchronized NRK cells were injected with Sar1dn protein 5 to 6 hours before entry into mitosis, to trap the Golgi enzymes in the ER, leaving the matrix proteins behind. Matrix fragments containing GM130 partitioned at all stages of mitosis in a manner almost indistinguishable from that of untreated cells. Partitioning occurred in the absence of ManII, which was present throughout the ER (Fig. 4).

These two experimental methods for separating Golgi enzymes and Golgi matrix proteins emphasize a partitioning mechanism that is independent of the ER. This mechanism depends on Golgi matrix structures rather than the enzyme-containing membranes that normally populate them, which in turn suggests that these membranes are a less important part of the Golgi partitioning process. They could either travel with the matrix structures to the daughter cells (as we would argue) or get there via the ER (as would be argued by others). Thus, the two models are no longer mutually exclusive, and one could imagine that enzymes could take either or both routes. In this context, recent work on budding yeast suggests that the early Golgi is inherited via the ER, whereas the late Golgi is inherited autonomously (*30*). In the end, it may not matter how the enzymes are inherited, provided that there is accurate inheritance of the Golgi matrix (*31*).

References and Notes

1. D. T. Shima, N. Cabrera-Poch, R. Pepperkok, G. Warren, *J. Cell Biol.* **141**, 955 (1998).
2. E. Jokitalo, N. Cabrera-Poch, G. Warren, D. T. Shima, *J. Cell Biol.* **154**, 317 (2001).
3. S. A. Jesch, A. J. Mehta, M. Velliste, R. F. Murphy, A. D. Linstedt, *Traffic* **2**, 873 (2001).
4. J. M. Lucocq, E. G. Berger, G. Warren, *J. Cell Biol.* **109**, 463 (1989).
5. K. J. Zaal *et al.*, *Cell* **99**, 589 (1999).
6. S. A. Jesch, A. D. Linstedt, *Mol. Biol. Cell* **9**, 623 (1998).
7. M. Terasaki, *Mol. Biol. Cell* **11**, 897 (2000).
8. S. R. Pfeffer, *J. Cell Biol.* **155**, 873 (2001).
9. J. Seemann, E. Jokitalo, M. Pypaert, G. Warren, *Nature* **407**, 1022 (2000).
10. T. H. Ward, R. S. Polishchuk, S. Caplan, K. Hirschberg, J. Lippincott-Schwartz, *J. Cell Biol.* **155**, 557 (2001).
11. A. Girod *et al.*, *Nature Cell Biol.* **1**, 423 (1999).
12. B. Storrie *et al.*, *J. Cell Biol.* **143**, 1505 (1998).
13. S. Miles, H. McManus, K. E. Forsten, B. Storrie, *J. Cell Biol.* **155**, 543 (2001).
14. Time-lapse phase images were acquired at 1-min intervals of synchronized NRK cells (*27*). Phase and fluorescence images were acquired with a Zeiss Axiovert 100M microscope equipped with an Orca 100 charge-coupled device camera (Hamamatsu, Hamamatsu City, Japan) and quantified with the program Openlab 3.0 (Improvision, Coventry, UK) (*32*, *33*).
15. Monoclonal antibodies used were as follows: NN2C10 (N. Nakamura) and 4A3 (M. Lowe) against GM130, GTL2 against β-1,4 galactosyltransferase (T. Suganuma), OKT8 against CD8 (F. Watt), TAT-1 against α-tubulin (K. Gull), 53FC3 against ManII (B. Burke), and 10C3 against KDEL (Stressgen, Victoria, Canada). Polyclonal antibodies used were as follows: GM130 (M. Lowe), mSec31p (F. Gorelick), GRASP65 (Y. Wang), calnexin (A. Helenius), myc (Santa Cruz, Santa Cruz, CA), and PDI (Stressgen). Alexa Fluor–conjugated secondary antibodies and To-Pro3 iodine were obtained from Molecular Probes (Eugene, OR). Secondary antibodies conjugated to horseradish peroxidase were purchased from Biosource (Camarillo, CA).
16. For confocal analysis, unsynchronized NRK cells were treated with BFA (5 μg/ml) (Epicentre, Madison, WI) for 90 min, fixed in −20°C methanol, and processed for immunofluorescence microscopy. Triple-labeled images were acquired on a Zeiss LSM510 microscope with a C-Apochromat 63x/1.2w Korr objective using the sequential (tracking) collection mode, and single sections (0.45 μm) in the *z* axis were collected.
17. J. Seemann, G.Warren, unpublished results.
18. R. R. Klevecz, *Methods Cell Biol.* **10**, 157 (1975).
19. HeLa cells stably expressing NAGTI-myc (*34*) were synchronized with 1 mM thymidine (Sigma) and treated with BFA, and mitotic cells were collected 90 min later by shake-off (*18*). After homogenization (*35*), the PCS was centrifuged on a 5 to 25% glycerol gradient [in 10 mM Hepes/KOH (pH 7.4) and 1 mM EDTA] over an 80% sucrose cushion (*3*, *6*). Fractions were collected and membranes were pelleted and processed for Western blot analysis. Alternatively, the PCS was centrifuged for 30 min at 110,000*g* to separate the membrane and cytosolic components, which were processed for Western blotting. Magnetic beads [Pan mouse immunoglobulin G (IgG) beads; Dynal, Oslo, Norway] coated (or not) with the monoclonal antibody 4A3 against GM130 were incubated with a PCS from mitotic NRK cells, synchronized using thymidine, and isolated by shake-off. Equal fractions (10%) of the supernatant and pellet were processed for Western blotting.
20. F. A. Barr, M. Puype, J. Vandekerckhove, G. Warren, *Cell* **91**, 253 (1997).
21. N. Nakamura *et al.*, *J. Cell Biol.* **131**, 1715 (1995).
22. P. Marra *et al.*, *Nature Cell Biol.* **3**, 1101 (2001).
23. S. Yoshimura *et al.*, *J. Cell Sci.* **114**, 4105 (2001).
24. A. T. Hammond, B. S. Glick, *Mol. Biol. Cell* **11**, 3013 (2000).
25. A. R. Prescott *et al.*, *Traffic* **2**, 321 (2001).
26. NRK cells were processed for Epon epoxy resin sections and immunolabelling as described (*33*).
27. M. Lowe, N. K. Gonatas, G. Warren, *J. Cell Biol.* **149**, 341 (2000).
28. Sar1dn was injected into the cytoplasm at 0.7 to 1 mg of protein per ml, together with sheep IgG (Sigma) to identify injected cells (*33*). Metaphase cells were injected 90 min after treatment with BFA (5 μg/ml). To analyze protein transport, metaphase cells were injected with a plasmid encoding CD8 (pCD8) (*1*) or a mixture of Sar1dn protein and pCD8. BFA was washed out after 1 hour, the cells were incubated for 2 hours at 37°C, and cycloheximide (0.1 mg/ml) (Sigma) was added 45 min before fixation.
29. Plasmids encoding mammalian Sar1dn mutants were kindly provided by W. E. Balch, and proteins were purified as described (*9*, *36*).
30. O. W. Rossanese *et al.*, *J. Cell Biol.* **153**, 47 (2001).
31. L. Pelletier, E. Jokitalo, G. Warren, *Nature Cell Biol.* **2**, 840 (2000).
32. R. Pepperkok *et al.*, *Cell* **74**, 71 (1993).
33. J. Seemann, E. Jämsä Jokitalo, G. Warren, *Mol. Biol. Cell* **11**, 635 (2000).
34. C. Rabouille *et al.*, *J. Cell Sci.* **108**, 1617 (1995).
35. W. E. Balch, J. E. Rothman, *Arch. Biochem. Biophys.* **240**, 413 (1985).
36. T. Rowe, W. E. Balch, *Methods Enzymol.* **257**, 49 (1995).

37. We thank J. Shorter, H. Meyer, L. Pelletier, and the Warren/Mellman lab for helpful discussions and K. Zichichi for technical assistance. Funded by a grant from NIH (to G.W.). T.T. was funded by postdoctoral fellowships from the Uehara Memorial Foundation and the Japan Society for the Promotion of Science (for Research Abroad).

15 November 2001; accepted 19 December 2001

Role of *Escherichia coli* Curli Operons in Directing Amyloid Fiber Formation

Matthew R. Chapman,[1] Lloyd S. Robinson,[1] Jerome S. Pinkner,[1] Robyn Roth,[2] John Heuser,[2] Mårten Hammar,[3] Staffan Normark,[3] Scott J. Hultgren[1]*

Amyloid is associated with debilitating human ailments including Alzheimer's and prion diseases. Biochemical, biophysical, and imaging analyses revealed that fibers produced by *Escherichia coli* called curli were amyloid. The CsgA curlin subunit, purified in the absence of the CsgB nucleator, adopted a soluble, unstructured form that upon prolonged incubation assembled into fibers that were indistinguishable from curli. In vivo, curli biogenesis was dependent on the nucleation-precipitation machinery requiring the CsgE and CsgF chaperone-like and nucleator proteins, respectively. Unlike eukaryotic amyloid formation, curli biogenesis is a productive pathway requiring a specific assembly machinery.

Bacteria express a variety of cell-surface proteinacious filaments that can promote colonization of an epithelial surface, entry into host cells, exchange of DNA between bacteria, and development of bacterial communities organized as biofilms, colonies, or multicellular fruiting bodies. Curli are a class of highly aggregated, extracellular fibers expressed by *Escherichia* and *Salmonella* spp. that are involved in the colonization of inert surfaces and